ChemComm

Accepted Manuscript

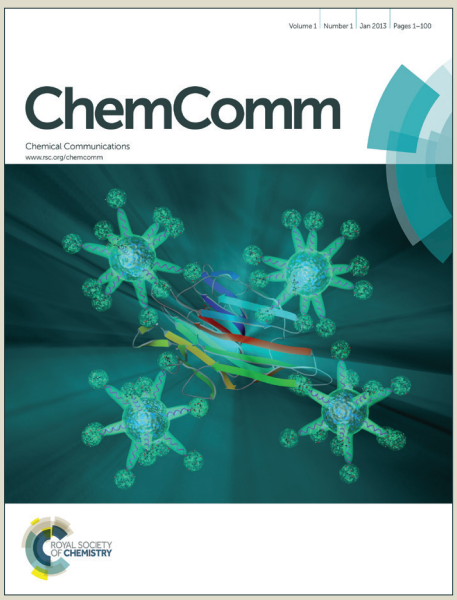

ROYAL SOCIETY OF CHEMISTRY

www.rsc.org/chemcomm

Cite this: DOI: 10.1039/c0xx00000x

www.rsc.org/xxxxxx

ARTICLE TYPE

The Nanoscale Carbon *p-n* Junction between Carbon Nanotube and N, B-Codoped Holey Graphene Enhances the Catalytic Activity towards Selective Oxidation

Hong Wang, Xiaoli Zheng, Haining Chen, Keyou Yan, Zonglong Zhu, Shihe Yang*

Received (in XXX, XXX) Xth XXXXXXXXX 20XX, Accepted Xth XXXXXXXXX 20XX
DOI: 10.1039/b000000x

We show spontaneous formation of multiple nanoscale carbon *p-n* junctions between carbon nanotubes (CNTs) and negatively charged N, B-codoped graphene (NBG). Application of these carbon nanocomposites to catalyze the selective oxidation of an organic amine to imine resulted in an unprecedented activity under mild conditions.

Aerobic oxidative coupling reactions that afford valuable organic compounds are of great importance in view of resource utilization and green chemistry[1]. The key step in this type of reactions is that the catalysts must have the strong ability to activate oxygen molecule[2]. Thus far, a variety of organic and inorganic catalysts[1a, 3], have been developed for the oxidation of organic molecules. These catalysts, however, typically suffer from low activity/selectivity[4], inadequate stability, need for co-catalyst[2c], high-cost, toxicity and limited resource[5]. More recently, heteroatom doped carbon nanomaterials have been recognized as promising metal-free and heterogeneous catalysts in organic synthesis and fuel cells, and are being heavily studied due to their relatively low cost, high natural abundance and their potentially comparable activity to the commercial platinum catalysts[6].

Herein we report a facile yet efficient route to prepare a novel type of carbon catalysts by exploiting the π-π and charge transfer interactions between 1D CNTs and 2D negatively charged NBG (see supporting information for synthesis details). Notably, multiple nanoscale carbon *p-n* junctions between the CNTs and the NBG were spontaneously formed, which support charge separation with potentially improved functionalities. Correlatively, the nanocomposite of 1D and 2D carbons is hierarchically structured forming an interpenetrating network. Such an interesting nanostructured material may find wide applications in chemical and electrochemical catalysis[7]. To demonstrate its catalytic power, we chose an oxidative coupling conversion reaction from amines to imines, which are highly useful intermediates for organic synthesis.

Scheme 1 illustrates the procedure for the nanoscale hybridization of the 1D CNTs and the 2D NBG with the resulting hierarchical interpenetrating network structure. By virtue of the π-π interaction between the CNTs and the NBG, the hybrid colloid can be formed with the assistance of sonication. Simultaneously, charge transfer takes place from the electron-rich CNTs to the electron-deficient NBG stemming from the N- and B-doping, creating multiple nanoscale carbon *p-n* junctions and synergistically aiding in the colloidal dispersion

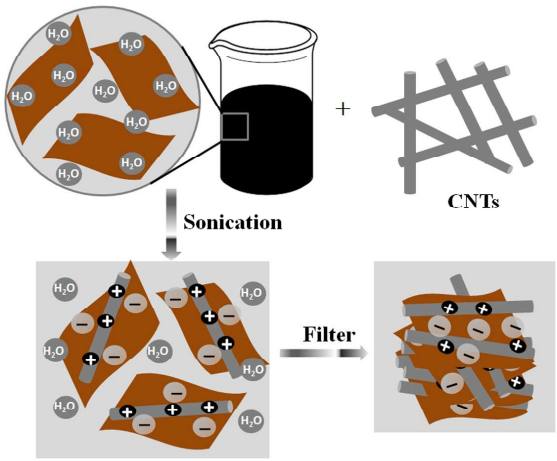

Scheme 1 Schematic illustrating the formation process of the NBG/CNTs nanocomposite - a 1D-2D hybrid structured, interpenetrating carbon network.

The presence of N, B elements in the graphene framework was revealed by X-ray photoelectron spectroscopy (XPS) analysis (Fig. S1). The N and B contents in BNG are as high as 17 atom% and 14 atom%, respectively. The N 1s XPS spectrum of NBG (Figure S1c) shows that the N atoms are inserted into the graphene framework mainly in the "pyridinic" (399.1 eV), "graphitic" (400.2 eV) and N-B (398.2 eV) forms. The population of the three forms of N atoms in NBG are about 35%, 44% and 21%, respectively. The B 1s XPS peaks (Figure S1d) at around 191.0 eV and 190.3 eV indicate the formation of N-B and C-B bonds[6a]. The peak at 191.9 eV is assigned to the terminal B-O bonds. The content of B atoms bonded with O is 41%, indicating that a large amount of B atoms are present on the edges of the graphene layers. Furthermore, from Fig. S1a and S1e, O species are present in the NBG sample, which can be attributed to strongly adsorbed oxygen-containing moieties, such as O_2 and CO_2 and H_2O. The observation of the O-containing species on the NBG sample actually underscores its high activity towards oxidation when exposed to air or water. The XPS results suggest that the graphene framework is heavily doped with the heteroatoms (N and B). The holey structure of the NBG can be

clearly seen from HRTEM images (Fig. S2), which could provide pathways for efficient mass transfer and thus may prove useful in the catalytic field[6a]. One striking characteristic of the NBG is their high dispersity in aqueous solutions to form a stable colloid without the assistance of any other stabilizers (Fig. S3). This can be attributed to the spontaneous charge transfer, hydroxyl adsorption and the super-thin structure (See TEM image in Fig. S4, supporting information) [8].

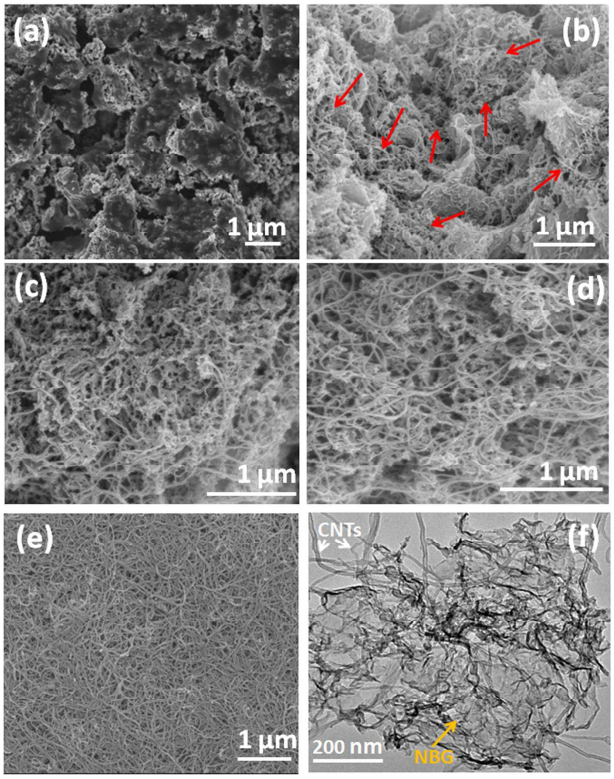

Fig. 1 SEM images of (a) pristine NBG, (b) NBG/CNTs (10:1), (c) NBG/CNTs (5:1), (d) NBG/CNTs (1:1), and (e) pristine CNTs. (f) HRTEM image of NBG/CNTs (5:1). The red arrows in (b) indicate the nanopores generated when the CNTs were hybridized with the NBG.

Fig. 1 shows representative scanning electron microscopy (SEM) images of the pristine NBG and the NBG/CNTs nanocomposites. It is clearly seen that the pristine NBG sheets are stacked (Figure 1a), whereas the NBG/CNTs(X) (X indicates the weight ratio of NBG to CNTs) nanocomposites appear to be more loose and fleecy. Indeed, an interpenetrating network structure was created via the π-π and charge transfer interactions, a kind of synergistic cross-linking, between the CNTs and the NBG upon sonication. When a small amount of CNTs was added, some nanoporous features already appeared (NBG/CNTs (10:1), Figure 1b) although the main component is still NBG. When the CNTs content was increased to NBG/CNTs (5:1), a typical interpenetrating network structure was resulted (Fig. 1c). This three-dimensional (3D) carbon network was formed by cross-linking the 1D CNTs with the 2D NBG. On further increase of the CNTs content, one can observe many bare CNTs (Fig. 1d), meaning that the interaction between NBG and CNTs has been reduced. Notably, all of the nanocomposites show good mixing of the components and there is no sign of macroscopic phase separation, which is clearly due to the strong π-π and charge-transfer interactions. Compared to the incompact structure of NBG/CNTs nanocomposites, the pristine CNTs appear to be more close-knit (Fig. 1e). The former is a novel 3D carbon network structure stemming from the hybridization of the 1D CNTs and the 2D NBG. From the high-resolution transmission electron microscopy (HRTEM) analysis (Fig. 1e), we can clearly see that the CNTs are cross-linked with the basal planes of NBG, mediated by the special π-π and/or charge transfer interactions between the 1D CNTs and the 2D NBG. Further support for such nanoscale hybridization was from the Brunauer-Emmett-Teller (BET) surface area measurement. The pristine NBG and CNTs have a specific surface area of 217 and 174 m^2g^{-1}, respectively. Surprisingly, the BET surface area of NBG/CNTs (10:1), NBG/CNTs (5:1) and NBG/CNTs (1:1) was dramatically increased to 339, 398 and 326 m^2g^{-1}, respectively (Fig. S5). This can only be explained if the 1D CNTs and the 2D NBG are successfully hybridized on the nanometer scale so that self-aggregation is prevented. Indeed, in agreement with the electron microscopic observations above, the NBG/CNTs (5:1) nanocomposite exhibits the highest surface area presumably because about the maximum possible cross-linking points have been achieved through the formation of the interpenetrating carbon networks.

To verify the formation of *p-n* junction between the electron-rich CNTs and the electron-deficient NBG, electrochemical impedance spectroscopy was performed at an AC frequency of 10 kHz in 1 M NaOH solution in a three-electrode photoelectrochemical cell. For this measurement, the nanocarbon samples were immobilized on a fluorine tin oxide (FTO) substrate to form a film working electrode. Representative Mott−Schottky (M−S) plots are shown in Fig. 3a and Fig. S6. For the NBG/CNTs (5:1) sample, the M-S plot (Fig. 3a) is characteristic of a *p*−*n* junction with an inverted "V-shape" [10]. In contrast, the M−S plots of the pristine CNTs and the pristine NBG show a positive slope (Fig. S6a) and a negative slope (Fig. S6b), respectively, indicating the corresponding n-type and p-type behaviors. We notice that CNTs can display both p-type and n-type behaviors. However, in n-type CNTs, only the side walls about 100 nm from the tail ends showed the p-type behavior[11]. Under our experimental condition, n-type CNTs were obtained. As for the pristine NBG, the p-type character is presumably a result of the heavy B-doping.

The *p-n* junction can effectively maintain the charge separation, which is very useful for catalysis as will be described below. Additional support for the unusual 1D carbon – 2D carbon *p*−*n* junction was obtained from zeta potential measurements. The pristine NBG surface is highly negatively charged when dispersed in water (-30.87 mV at room temperature), making its dispersion fairly stable in aqueous solution. To our surprise, the zeta potentials measured for the upper stable NBG/CNTs (10:1) and NBG/CNTs (5:1) dispersions were -32.37 mV and -40.90 mV, respectively. This suggests that charge transfer has occurred from the electron rich CNTs to the electron deficient NBG arising from the B, N-doping. More specifically, electron is transferred from the CNTs to the NBG while hole moves from the NBG to the CNTs, creating a "depletion region" near the junction, and at a certain stage the built-in potential blocks further electron flow. As a result, the negative charge on the NBG surface will be

increased, and this explains why the zeta potential of the NBG/CNTs (10:1) nanocomposite (-32.37 mV) and NBG/CNTs (5:1) nanocomposite (-40.09 mV) is higher than that of the pure NBG (-30.87 mV). Such charge transfer adds the electrostatic attraction to the already present π-π interaction between the 1D CNTs and the 2D NBG, and strengthens the multiple carbon *p*–*n* junctions.

Photoluminescence (PL) measurements were also carried out on the NBG/CNTs nanocomposites since PL can often provide important information about the junction interfaces[12]. The PL spectra of the NBG/CNTs nanocomposites with various composition are shown in Fig. 3b. As a benchmark, the PL spectrum for NBG is characterized by a broad intense peak at around 600 nm, whereas barely luminescent features were observed for the CNTs. The most important finding is the drastic reduction of the PL intensity of the NBG/CNTs nanocomposites compared with that of the pristine NBG even when a small amount of CNTs was introduced. Moreover, the PL quenching increases with increasing CNTs content in nanocomposites. Such PL quenching appears to be caused by the transfer of the holes from NBG to the CNTs driven by the built-in potential of the carbon *p*–*n* junction between them and thus the significantly reduced radiative recombination between the excited electrons and holes. Therefore the PL result supports the multiple carbon *p*-*n* junctions formed between the NBG and the CNTs.

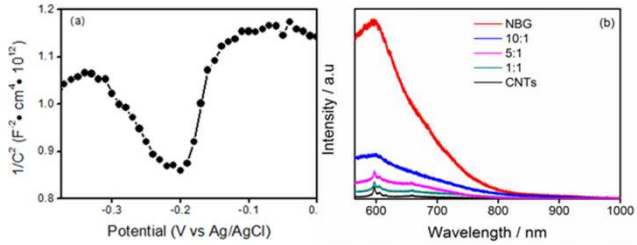

Fig. 3 (a) Mott−Schottky plot of the NBG/CNTs (5:1) sample obtained in 1M NaOH solution using a three-electrode photoelectrochemical cell; (b) Photoluminescence spectra of NBG, NBG/CNTs (10:1), NBG/CNTs (5:1), NBG/CNTs (1:1), and CNTs with an excitation laser line at 514 nm

Our initial studies focused on the oxidative coupling of benzylamine to imine catalyzed by the NBG/CNTs nanocomposites. The catalytic performance result is summarized in Table 1. In isolation, NBG is catalytically active towards the reaction whereas CNTs is inactive. Remarkably, when a small amount of CNTs is hybridized with NBG, the catalytic activity is significantly increased. However, this increase in catalytic activity is followed by a decrease when too much CNTs is introduced. Two important factors are held responsible for the composition dependent catalytic activity of the NBG/CNTs nanocomposites: the BET surface area and the amount of the *p*-*n* junctions. When a small amount of CNTs was added, the surface area was significantly increased, resulting in a similar increase in the catalytic activity. However, too much CNTs actually reduced the catalytic activity of the nanocomposites owing to the decreased amounts of the active material (NBG). With a weight ratio of NBG to CNTs is 5:1, the NBG/CNTs (5:1) nanocomposite exhibited the highest catalytic activity, presumably due to its highest BET surface area resulting from the hierarchical interpenetrating network structure and the maximum possible number of nanoscale *p*-*n* junctions. Such a structure is beneficial to the diffusion of reactants and products inside the nanopores while the multiple nanoscale *p*-*n* junctions may assist in the activation of the reactants and the separation of the products. According to the proposed mechanism, the first step of this type of reaction is to activate the oxygen molecule (O_2). The electrons are transferred from the NBG to O_2, forming O_2^-, which will then combine with H^+ in amine to release a H_2O and/or H_2O_2 molecule[6]. In our designed nanocomposite, the net electron density on the NBG surface in the NBG/CNTs (5:1) nanocomposite is much higher than in the pristine NBG due to the effect of the *p*-*n* junctions. Therefore, O_2 can be more efficiently activated on the NBG surface in the NBG/CNTs (5:1) nanocomposite, resulting in the significantly improved catalytic activity we observed.

Table 1. Performance of various carboncatalysts for the oxidative coupling of benzylamine to imine.[a]

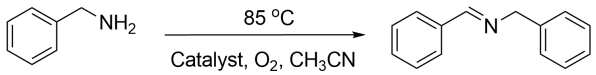

Entry	Catalyst	Conversion %[b]	Selectivity %[b]
1	NBG	72	>99
2	NBG/CNTs(10:1)	85	>99
3	NBG/CNTs(5:1)	92	>99
4	NBG/CNTs(1:1)	64	>99
5	CNTs	-	-

[a] Standard reaction conditions: acetonitrile (5 mL), substrate (1 mmol), catalyst (30 mg), O_2 balloon (1 atm), 3 h, 85°C. [b] The conversion and selectivity were determined by GC–MS using aniline as the internal standard

Finally, we have shown that our carboncatalyst is also effective in the aerobic oxidative coupling of amines with different substituents (see Table 2) under the mild condition (acetonitrile (5 mL), substrate (1 mmol), catalyst NBG/CNTs(5:1) (30 mg), O_2 balloon (1 atm), 3 h, 85 °C**)**. Table 2 exemplifies the scope and the versatility of the carboncatalyst. It is noted that NBG/CNTs (5:1) could activate O_2 for the transformation of the amines into an imines with very high selectivity (>99%). With a combination of the high activity, the high selectivity and the stable reuseability (after five cycles, there was no obvious loss of catalytic activity, Fig S7), the carboncatalyst shows a great potential for applications in the aerobic oxidative coupling reactions.

Table 2. Performance summary of the NBG/CNTs (5:1) catalyst for the oxidative coupling reaction of various amines

Entry	Substrates	Products	Conv. [%]	Sele. [%]
1	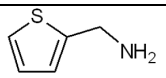	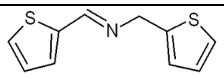	62	>99
2	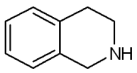	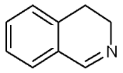	92	>99
3	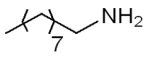	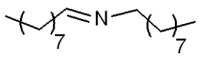	28	>99

Conclusions

In conclusion, we have created the multiple carbon *p*-*n* junctions

between 1D CNTs and 2D NBG, both of which are sp^2-based carbon materials by virtue of the π-π stacking and the charge transfer interactions. Owing to the increased specific surface area arising from the 1D-2D hybridization and the purported charge separation stemming from carbon *p-n* junctions, the hybrid carboncatalysts showed high activity, high selectivity and excellent reusability towards the oxidative coupling of amine to imine. It is anticipated that the interpenetrating carbon network structure made up of the high conductivity carbon materials in combination with the pronounced charge separation will find many practical applications such as in electrode materials, electrocatalysts, and gas sensors. This work validates the composite approach to the design and fabrication of new types of functional materials.

This work was financially supported by the HK-RGC General Research Funds (GRF Nos. HKUST 605710 and 6046511)

Notes and references

Department of Chemistry, The Hong Kong University of Science and Technology, Clear Water Bay, Kowloon, Hong Kong, P. R. China, E-mail: chsyang@ust.hk

†Electronic Supplementary Information (ESI) available: Synthesis and characterization details for the resulted sensitizers. See DOI: 10.1039/b000000x/

[1] (a) T. Punniyamurthy, S. Velusamy, J. Iqbal, *Chem. Rev*. 2005, **105**, 2329-2363; (b) Y.-Q. Zou, J.-R. chen, Xiao-Peng Liu, L.-Q. Lu, R. L. Davis, K. A. Jørgensen, W.-J. Xiao, *Angew. Chem. Int. Ed*. 2012, **124**, 808-812.

[2] S.-I. Murahashi, T. Nakae, H. Terai, N. Komiya, *J. Am. Chem. Soc.* 2008, **130**, 11005-11012.

[3] M. J. Schultz, M. S. Sigman, *Tetrahedron*, 2006, **62**, 8227-8241.

[4] H. Tsunoyama , H. Sakurai , Y Negishi , T. Tsukuda, *J. Am. Chem. Soc.* 2005, **127**, 9374-9375.

[5] L. Ackermann, L. T. Kaspar, *J. Org. Chem.* 2007, **72**, 6149-6153.

[6] (a) X.-H. Li, M. Antonietti, *Angew. Chem. Int. Ed.* 2013, **52**, 4572-4576; (b) C. Su, M. Acik, K. Takai, J. Lu, S.-J. Hao, Y. Zheng, P. Wu, Q. Bao, T. Enoki, Y. J. Chabal, K. P. Loh, *Nat. Comm.* 2012, **3**, DOI: 10.1038/ncomms2315.

[7] (a) Y. H. Bing , S. Liu , L. Zhang , D. Ghosh , J. J. Zhang , Chem. Soc. Rev. 2010, 39, 2184-2202; (b) G. Milczarek, O. Inganäs, *Science* 2012, **335**, 1468-1471.

[8] D. Kuzmicz, S. Prescher, F. Polzer, S. Soll, C. Seitz, M. Antonietti, J. Yuan, *Angew. Chem. Int. Ed.* 2014, **126**, 1080-1084.

[9] X.-H. Li, S. Kurasch, U. Kaiser, M. Antonietti, *Angew. Chem. Int. Ed.* 2012, **51**, 9689-9692.

[10] F. Meng, J. Li, S. K. Cushing, M. Zhi, N. Wu. *J. Am. Chem. Soc.* 2013, **135**, 10286-10289.

[11] J. Parka and P. L. McEuena, *Appl. Phys. Lett.* 2001, **79**, 1363, 1363-1365.

[12] Y. Yu, J. C. Yu, C.-Y. Chan, Y.-K. Che, J.-C. Zhao, L. Ding, W.-K. Ge, P.-K. Wong, *Appl. Cata., B* 2005, **61**, 1-11.